Electronic Journal of University of Aden for Basic and Applied Sciences

EJUA-BA Vol. 6 No. 4 (2025)

https://doi.org/10.47372/ejua-ba.2025.4.474

ISSN: 2708-0684

RESEARCH ARTICLE

EVALUATION OF GAMMA AND FAST NEUTRON SHIELDING PROPERTIES OF YEMENI BUILDING MATERIALS

Sawsun Abdallah Mohammed[1], Maher Taher Hausain[2], and Emran Eisa Saleh[3,*]

[1] *Dept. of Physics, Faculty of Education, University of Aben, Yemen*
[2] *Dept. of Physics, Faculty of Education Yafea, University of Lehj, Yemen*
[3] *Dept. of Physics, Faculty of Science, University of Aden, Yemen*

***Corresponding author: Emran Eisa Saleh; E-mail: eesas2009@yahoo.com**

Received: 05 October 2025 / Accepted: 01 December 2025 / Published online: 31 December 2025

Abstract

This study evaluated the gamma radiation shielding properties of eight Yemeni rock samples (A0, A1, A2, B0, B1, R0, R1, and R2) across photon energies from 0.015 to 15 MeV. Key nuclear shielding parameters—including mass attenuation coefficient (MAC), half-value layer (HVL), mean free path (MFP), and effective atomic number (Z_{eff})—were calculated. Among the samples, A0 and R1 exhibited the best shielding performance, with MAC values reaching 21.0 and 21.4 cm^2/g at 0.015 MeV, surpassing conventional materials such as ordinary concrete and commercial glasses Rs-360 and Rs-253 G18. Corresponding HVL values were as low as 0.045 cm for A0 and 0.042 cm for R1, indicating effective attenuation with minimal thickness. Low MFP values further confirm the high gamma photon interaction efficiency of these samples. Their Zeff values peaked near 20 at low energies, reflecting significant elemental contributions to photon absorption. Collectively, these results demonstrate that rock samples A0 and R1 offer superior gamma radiation shielding, requiring thinner layers to achieve comparable protection relative to traditional materials. Additionally, Macroscopic removal cross-section (ΣR) values ranged from 0.034 to 0.075 cm^{-1}, with sample A1 showing superior fast neutron shielding efficiency. Interestingly, ΣR decreased as sample density increased. This highlights their potential as cost-effective, naturally sourced shielding materials suitable for nuclear safety and construction applications.

Keywords: Gamma shielding; Attenuation; Atomic number; Rocks; HVL.

1. Introduction:

The study of interactions between high-energy photons and matter is fundamental in various fields including radiation medicine, nuclear technology, shielding design, and space research [1-3]. Gamma rays interact with materials primarily through absorption, scattering, and transmission processes. A precise understanding of these interactions is crucial in applications such as radiation dosimetry, medical imaging, and crystallography [4-6].

The mass attenuation coefficient (MAC) quantifies the probability of interaction between incident photons and a material per unit mass thickness, serving as a key parameter in describing the attenuation and transmission behavior of X-rays and gamma rays within materials. Measurement of gamma ray attenuation coefficients and cross-sections provides valuable information for applications like computerized tomography and radiation biology. In complex media, the effective atomic number (Zeff) and effective electron density (Neff) represent unique quantities used to characterize photon energy absorption more accurately [7-11].

Accurate evaluation of these parameters is essential for the selection and development of suitable radiation shielding materials [12]. Moreover, reliable data on mass attenuation coefficients (μ/ρ), atomic cross-section (σ_e), effective atomic number, and electron density are critical for various scientific and engineering applications. These parameters have been extensively investigated in a wide range of materials, including alloys, biological tissues, and natural minerals across different energies [13-18].

The objective of this manuscript is to experimentally investigate the gamma radiation shielding properties of selected materials used in Yemen, focusing on key

parameters such as MAC, LAC, HVL, and Z_{eff}. This study aims to provide accurate attenuation data, structural analysis, and comparative performance insights to evaluate the suitability of these materials for effective gamma and neutron radiation shielding applications.

2.Materials and method:

2.1. Sample Preparation

Building material samples were collected from various governorates in Yemen. After collection, the samples were ground into fine powder to facilitate analysis by X-ray fluorescence (XRF), which was used to determine the oxide composition of each sample.

A total of eight environmental rock samples intended for use as building materials were gathered: four from Abyan (labeled A0, A1, A2, and B0), two from Lahj (B1 and R0), one imported from Egypt (R1), and one from China (R2). The Egyptian and Chinese samples were specifically included to evaluate their potential as shielding materials against gamma and neutron radiation.

2.2. Characterization Techniques

Elemental analysis of the samples was performed using XRF to identify the oxide constituents. The density of the samples was measured at room temperature (25°C) using an electronic balance with a precision of 0.0001 g. Measurements were taken both in air and while buoyant in toluene. The density (ρ) was calculated using the following formula:

$$\rho = p_t W_{ga} / (W_{ga} - W_{at}) \text{ ……..(1)}$$

where (W_{ga}) is the weight of the sample in air, (W_{at}) is the weight of the sample in toluene, and (p_t) is the density of toluene (0.87 g/cm³).

2.3. Computational Methods

The nuclear radiation shielding parameters were computed using the online Photon Shielding and Dosimetry (PSD) software available at https://phy-x.net/PSD, alongside theoretical calculations obtained from the XCOM online program. Both tools were utilized to evaluate gamma ray shielding properties of the prepared samples [19].

3.Results and Discussion

In this study, eight different building material samples labeled A0, A1, A2, B0, B1, R0, R1, and R2 were prepared and examined for their potential use as gamma ray shields. The densities and chemical oxide compositions of these materials are summarized in Table 1. The densities ranged from 1.344 to 2.513 g/cm³, reflecting variability in sample composition and compactness.

Table 2 presents the mass attenuation coefficients (MAC) calculated using the PHY-X/PSD software across an energy range of 0.015 to 15 MeV. Figure 1 illustrates MAC variation with energy. The mass attenuation coefficient (MAC) values for the eight rock samples (A0, A1, A2, B0, B1, R0, R1, and R2) were calculated across photon energies ranging from 0.015 MeV to 15 MeV. The MAC values generally decrease with increasing photon energy, consistent with the known behavior of photon interactions with matter.

At the lowest energy (0.015 MeV), all samples show the highest MAC values, with values ranging from approximately 12.78 cm²/g (A1) to 21.39 cm²/g (R1). This trend reflects the dominance of the photoelectric effect at low photon energies, which is highly sensitive to the atomic number and density of the material. Samples R1, R0, and A0 consistently exhibit the highest MAC values in this energy region, indicating their potentially higher effectiveness as gamma radiation shielding materials compared to others.

As energy increases (e.g., 0.02 MeV to 0.1 MeV), a sharp decline in MAC is observed across all samples, illustrating the transition from photoelectric absorption to predominantly Compton scattering interactions. Differences between samples become less pronounced at these intermediate energies, though R1 and R0 maintain slightly higher attenuation coefficients.

From about 0.3 MeV upwards, the MAC values slowly decrease and tend to plateau toward lower values (around 0.025 cm²/g at 15 MeV). In this energy range, Compton scattering is the dominant interaction and is less dependent on atomic number, explaining the reduced variation among samples.

Interestingly, sample A1 consistently shows lower MAC values across most energies, particularly at low energies, suggesting a lower average atomic number or density relative to other samples. Meanwhile, samples such as R1, R0, and A0 tend to maintain superior attenuation capabilities throughout the energy spectrum.

Overall, the MAC data indicate that while all examined rock samples demonstrate typical energy-dependent attenuation behavior, certain samples—specifically R1, R0, and A0—offer enhanced attenuation efficiency due to their higher MAC values at low and intermediate energies. These samples may thus serve as more effective options for gamma radiation shielding applications in construction or related fields.

The mass attenuation coefficient (MAC) provides the probability of gamma photon interaction per unit mass, but to assess practical shielding performance, it is important to consider related parameters such as the linear attenuation coefficient (LAC) and the half-value layer (HVL).

The LAC is directly related to the MAC through the material density (LAC = p × MAC), quantifying the probability of photon interaction per unit thickness of material. Since the examined rock samples exhibit densities ranging approximately from 1.344 to 2.513 g/cm³, differences in density further amplify variations observed in MAC values. Fig. 2, presents the LAC values versus energy for rocks samples. From the figure, samples like R1, R0, and A0, which showed higher MACs, will correspondingly exhibit higher LACs due to their relatively greater densities. This results in a greater capacity to attenuate gamma rays per unit thickness, making these rocks more effective as shielding materials.

The half-value layer (HVL), defined as the thickness required to reduce the gamma radiation intensity by 50%, is inversely related to the LAC (HVL = ln 2 / LAC). Thus, materials with higher LAC and MAC values will show a lower HVL, which translates to thinner shields required for effective attenuation. Fig. 3, presents the HVL for rocks samples with gamma energy.

In this study, rock samples with the highest MAC values at low energies—R1, R0, and A0—also demonstrated the lowest HVLs, illustrating their superior shielding capability. Conversely, samples with lower MAC and LAC (e.g., A1) require greater thicknesses to attenuate the same intensity of gamma radiation, as reflected by larger HVL values.

Energy dependence is also evident across these parameters. At low photon energies (<0.1 MeV), where photoelectric absorption dominates, stark differences in MAC, LAC, and HVL among the samples are observed due to variations in elemental composition and density. As photon energy increases, Compton scattering dominates, which depends less on atomic number but varies with electron density, causing attenuation parameters to converge and differences among samples to become less distinct.

In summary, the comparative analysis of MAC, LAC, and HVL confirms that rock samples R1, R0, and A0 possess favorable gamma radiation shielding characteristics due to their higher attenuation coefficients and densities, enabling thinner and more effective shielding solutions. This comprehensive assessment is crucial for selecting suitable materials in construction or nuclear protection applications.

To evaluate the practical significance of the shielding properties of rock samples A0 and R1, their mass attenuation coefficients (MAC) and half-value layers (HVL) were compared against commonly used standard shielding materials, including ordinary concrete (OC), barite concrete (BaC), chromium (Cr), iron (Fe), and commercial radiation shielding glasses Rs-360 and Rs-253 G18. Fig. 4 and 5, represent the MAC and HVL compared with standard shielding materials respectively.

At low photon energies (e.g., 0.015 MeV), both A0 and R1 demonstrated MAC values of approximately 21.0 and 21.4 cm²/g respectively, which are notably higher than those of ordinary concrete and commercial glasses such as Rs-360 and Rs-253 G18. This indicates a greater probability of photon interaction per unit mass in A0 and R1, suggesting their superior attenuation capability, especially when shielding against low-energy gamma rays.

Barite concrete, known for its higher density and enhanced shielding properties, typically exhibits MAC values closer to these rock samples at low energies. However, A0 and R1 often remain competitive or outperform barite concrete in specific energy ranges, particularly below 0.1 MeV due to their unique composition and density.

Compared to elemental standards such as chromium and iron, which are commonly referenced for their attenuation properties, A0 and R1 show favorable MAC values at similar energies, reflecting the advantage of natural composite materials with high effective atomic numbers.

The HVL values complement MAC results by showing the thickness of material required to reduce gamma ray intensity by half. Lower HVL values indicate more efficient shielding per unit thickness. At 0.015 MeV, sample R1 exhibited an HVL of approximately 0.042 cm, which is significantly lower compared to ordinary concrete and commercial glasses, implying that thinner shields of R1 can provide equivalent or better protection.

Sample A0 also showed remarkably low HVL values, closely matching or outperforming some barite concrete ranges in parts of the energy spectrum, specifically in the 0.04 to 0.08 MeV range. Commercial glasses, while providing certain optical benefits, generally require greater thicknesses to achieve the same attenuation level as these rock samples.

The mean free path (MFP) represents the average distance photons travel within a material between successive interactions. It is inversely proportional to the linear attenuation coefficient (LAC), which itself is derived from MAC multiplied by density. Thus, higher attenuation coefficients translate to shorter MFP values. Fig. 6. Represents the MFP versus photon energy. Samples A0 and R1, exhibiting high MAC values and correspondingly low HVLs, also show reduced MFPs, confirming their efficient gamma ray interaction and minimal penetration depth.

Shorter MFPs directly correlate with enhanced protective performance since radiation is more likely to be absorbed or scattered over shorter distances within these materials. The low MFP at energies where photoelectric absorption dominates (below ~0.1 MeV) particularly highlights the effectiveness of A0 and R1 in attenuating low-energy

gamma photons, a critical range for many radiation shielding applications.

The effective atomic number (Z_{eff}) is a weighted average representing the composite shielding material's ability to interact with photons and is closely related to photon interaction processes that depend on atomic number, such as photoelectric absorption. Typically, Z_{eff} peaks at lower photon energies due to the dominance of the photoelectric effect, which is highly sensitive to the presence of high-Z elements. Fig. 7. Represents the (Z_{eff}) with energy photon.

Samples A0 and R1 demonstrate relatively high Z_{eff} values compared to other tested materials, confirming the presence of high atomic number constituents contributing to their elevated MAC. This high Z_{eff} not only explains the better gamma attenuation at low energies but also supports improved scattering and absorption efficiencies over broad energy ranges.

For protection against fast neutrons—uncharged particles that interact differently—the macroscopic removal cross-section (Σ_R) was evaluated (Figure 8). Higher Σ_R values imply more efficient neutron attenuation through increased probability of neutron interactions. The Σ_R values ranged from 0.034 cm^{-1} (A0) to 0.075 cm^{-1} (A1). Interestingly, Σ_R decreased as sample density increased. Sample A1 showed superior neutron capture efficiency compared to others, with its Σ_R exceeding that of typical neutron.

4. Conclusion

Rocks are durable, sustainable building materials widely used in construction due to their natural strength and aesthetic variety. This study evaluated selected building materials for their effectiveness in shielding against gamma rays and fast neutrons over energies from 0.015 to 15 MeV. Using the PHY-X/PSD software, key radiation shielding parameters—including MAC, LAC, HVL, TVL, MFP, Zeff, Neff, and fast neutron removal cross-section—were calculated and compared with standard materials like concrete and commercial glass.

Sample densities ranged from 1.344 to 2.513 g/cm^3. Sample A1 showed the highest fast neutron removal cross-section (0.075 cm^{-1}), while R1 and R0 exhibited superior gamma shielding with MAC values around 21 cm^2/g and LAC values up to 53.7 cm^{-1} at 15 keV. Samples R1 and R2 had the lowest HVL and TVL, indicating excellent attenuation performance. Zeff peaked at over 20 for certain samples, highlighting their strong photon interaction capacity.

These findings demonstrate that some of the studied building materials, especially A1 and R1, offer promising radiation shielding properties, potentially outperforming conventional materials in nuclear protection applications.

References:

[1] D. Taya, A. Saeed, and E. E. Saleh, "Evaluation of nuclear radiation shielding behavior and structure properties of novel B2O3-Na2O-K2O-xBi2O3 glasses," EJUA, vol. 4, no. 4, pp. 305–313, 2023, doi: 10.47372/ejua-ba.2023.4.296.

[2] M. A. Algradee, E. E. Saleh, O. M. Samir, A. B. Alwany, and T. M. El-Sherbini, "Physical, structural, optical, and gamma ray shielding properties of Li2O–ZnO–SiO2–P2O5 glasses doped with Nd2O3," Appl. Phys. A, vol. 128, p. 1028, 2022, doi: 10.1007/s00339-022-06180-x.

[3] E. E. Saleh et al., "Synthesis and Nuclear Radiation Shielding Ability of Li2O-ZnO-P2O5 Glasses: The Role of Yb2O3," J. Electron. Mater., vol. 51, no. 12, p. 14, 2022, doi: 10.1007/s11664-022-09979-9.

[4] M. S. Al-Fakeh, E. E. Saleh, and F. Alresheedi, "Synthesis of Novel Li2O-CuO-Bi2O3-B2O3 Glasses for Radiation Protection: An Experimental and Theoretical Study," Inorganics, vol. 11, no. 1, p. 27, 2023, doi: 10.3390/inorganics11010027.

[5] M. N. Murshed et al., "Novel Li2O–BaO–PbO–B2O3 glasses: physical, structural, optical, gamma ray shielding, and fast neutron features," Opt. Quantum Electron., vol. 56, no. 4, 2024, doi: 10.1007/s11082-024-06304-y.

[6] M. A. Algradee et al., "Structural, physical and optical properties of ZnO-V2O5-P2O5 glass system," J. Non Cryst. Solids, vol. 589, p. 121664, 2022, doi: 10.1016/j.jnoncrysol.2022.121664.

[7] M. A. Algradee, A. A. Higazy, and S. Wageh, "Structural and Optical Properties of Li2O–NaF–ZnO–P2O5: (CdO+S) Glass System," J. Adv. Phys., vol. 5, pp. 1–8, 2016.

[8] E. E. Saleh et al., "Fabrication of novel lithium lead bismuth borate glasses for nuclear radiation shielding," Radiat. Phys. Chem., vol. 193, p. 109939, 2021, doi: 10.1016/j.radphyschem.2021.109939.

[9] M. A. Algradee et al., "Evaluation of structural, elastic properties and nuclear radiation shielding competence of Nd3+ doped lithium-zinc-phosphate glasses," J. Non Cryst. Solids, vol. 576, p. 121304, 2021, doi: 10.1016/j.jnoncrysol.2021.121304.

[10] E. E. Saleh, M. A. Algradee, and M. S. Al-Fakeh, "Nuclear radiation shielding behavior for prepared LNZP glasses doped with (CdO+Te)," Radiat. Phys. Chem., vol. 189, p. 109743, 2021, doi: 10.1016/j.radphyschem.2021.109743.

[11] M. A. Algradee et al., “Optical and gamma-ray shielding features of Nd3+ doped lithium-zinc-borophosphate glasses,” Optik, vol. 242, p. 167059, 2021, doi: 10.1016/j.ijleo.2021.167059.

[12] A. B. Alwany et al., “Effect of lead doping on the structural, optical, and radiation shielding parameters of chemically synthesized ZnS nanoparticles,” J. Mater. Sci.: Mater. Electron., vol. 34, no. 3, 2022, doi: 10.1007/s10854-022-09647-y.

[13] M. N. Brekhovskikh et al., “Synthesis and glass formation in the BaO-B2O3-BaCl2 system,” Inorg. Mater., vol. 46, no. 12, pp. 1391–1395, Dec. 2010, doi: 10.1134/S0020168510120216.

[14] Aboutaleb and Safi, “Structure and Properties of the Soda-Borate Glasses: Effect of Adding Fe2O3 Concentration,” J. Chem. Eng. Process Technol., vol. 7, no. 1, 2016, doi: 10.4172/2157-7048.1000268.

[15] A. M. Al-Esaei et al., “Estimation of effective doses to whole-bodies and hands of facilitating staff from radioiodine-131 ablation therapy patients,” Egypt J. Radiol. Nucl. Med., vol. 55, p. 60, 2024, doi: 10.1186/s43055-024-01241-y.

[16] A. M. Al-Esaei et al., “Evaluation of Radiation Safety Parameters from Patients Receiving I-131 Therapy for Thyroid Carcinoma,” J. Med. Phys. Appl. Sci., vol. 9, no. 1, p. 52, 2024.

[17] M. Algradee et al., “Electronic polarizability, optical basicity and interaction parameter for Nd2O3 doped lithium–zinc–phosphate glasses,” Appl. Phys. A, vol. 123, no. 524, pp. 1–12, 2017.

[18] E. E. Saleh et al., “Cd-S Doped Glass Shields: Structural, Optical, and Nuclear Shielding Characteristics,” Radiat. Phys. Chem., vol. 237, p. 112969, 2025, doi: 10.1016/j.radphyschem.2025.112969.

[19] Ö. F. Sakar et al., “Phy-X/PSD: development of a user friendly online software for calculation of parameters relevant to radiation shielding and dosimetry,” Radiat. Phys. Chem., vol. 166, p. 108496, 2020.

List of tables:

Table (1): displays the density, average molecular weight, as well as the oxides and elements for all the rocks examined in the study.

Type of rocks	Marble	Igneous	Igneous	Block	Red block	Marble	Marble	Metamorphic
Code	A0	A1	A2	B0	B1	R0	R1	R2
Density g/cm3	1.160	2.284	1.414	1.958	1.740	1.344	2.513	1.668
AMW g/mol	56.20	72.86	65.09	75.62	77.03	55.79	56.16	68.61
SiO2 %mol	2.83	54.91	31.85	46.67	41.94	2.46	2.67	7.07
Al2O3	1.19	14.96	6.67	13.42	13.44	1.09	1.09	2.29
Fe2O3	0.32	5.76	4.53	10.85	12.48	0.30	0.68	1.15
CaO	93.17	21.48	54.91	28.32	29.76	93.98	93.26	89.15
MgO	0.0	1.14	0.0	0.0	0.0	0.0	0.0	0.0
K2O	0.04	0.82	0.52	0.72	0.58	0.02	0.018	0.01
Na2O	0.0	3.45	0.0	0.0	0.0	0.0	0.0	0.0
SO3	0.15	0.16	0.62	0.012	0.23	0.16	0.04	0.23
Cl	0.012	0.022	0.400	0.0014	1.484	0.002	0.004	0.010
Si	0.014	0.168	0.120	0.146	0.131	0.012	0.013	0.032
O	0.514	0.609	0.582	0.610	0.603	0.509	0.511	0.525
Al	0.012	0.092	0.050	0.084	0.084	0.011	0.011	0.021
Fe	0.003	0.035	0.034	0.068	0.078	0.003	0.007	0.011
Ca	0.455	0.066	0.207	0.088	0.093	0.464	0.458	0.409
K	0.0004	0.003	0.004	0.005	0.005	0.0002	0.0006	0.0001
S	0.003	0.005	0.002	0.0	0.0007	0.0	0.0002	0.001
Na	0.0	0.021	0.0	0.0	0.0	0.0	0.0	0.0

Table (2): The mass attenuation coefficient (MAC) values for rock samples

Energy (MeV)	Mass attenuation coefficient cm2/g							
	Sample A0	A1	A2	B0	B1	R0	R1	R2
0.015	21.013	12.778	17.310	17.118	21.013	21.219	21.385	20.528
0.02	9.231	5.666	7.649	7.618	9.231	9.321	9.400	9.028
0.04	1.337	0.885	1.142	1.150	1.337	1.349	1.360	1.313
0.05	0.766	0.535	0.667	0.672	0.766	0.772	0.778	0.754
0.08	0.303	0.246	0.278	0.279	0.303	0.304	0.306	0.300
0.1	0.225	0.194	0.211	0..212	0.225	0.225	0.226	0.223
0.15	0.157	0.147	0.152	0.152	0.157	0.157	0.157	0.156
0.2	0.133	0.127	0.130	0.129	0.133	0.133	0.133	0.132
0.3	0.110	0..107	0.108	0.108	0.108	0.11	0.11	0.110
0.4	0.097	0.095	0.096	0.095	0.095	0.097	0.097	0.097
0.5	0.088	0.086	0.087	0.086	0.086	0.088	0.088	0.088
0.6	0.071	0.080	0.080	0.079	0.079	0.081	0.081	0.081
0.8	0.063	0.070	0.070	0.070	0.069	0.071	0.071	0.071
1	0.051	0.063	0.063	0.062	0.062	0.064	0.064	0.064
1.5	0.045	0.051	0.051	0.051	0.051	0.052	0.052	0.052
2	0.037	0.044	0.044	0.442	0.044	0.045	0.045	0.045
3	0.033	0.036	0.036	0.036	0.036	0.037	0.037	0.037
4	0.030	0.031	0.032	0.032	0.032	0.033	0.033	0.033
5	0.028	0.029	0.029	0.029	0.029	0.03	0.03	0.030
6	0.028	0.027	0.027	0.027	0.027	0.029	0.029	0.029
8	0.026	0.024	0.025	0.025	0.025	0.027	0.027	0.027
10	0.026	0.023	0.024	0.024	0.024	0.026	0.026	0.026
15	0.025	0.022	0.023	0.023	0.023	0.025	0.025	0.025

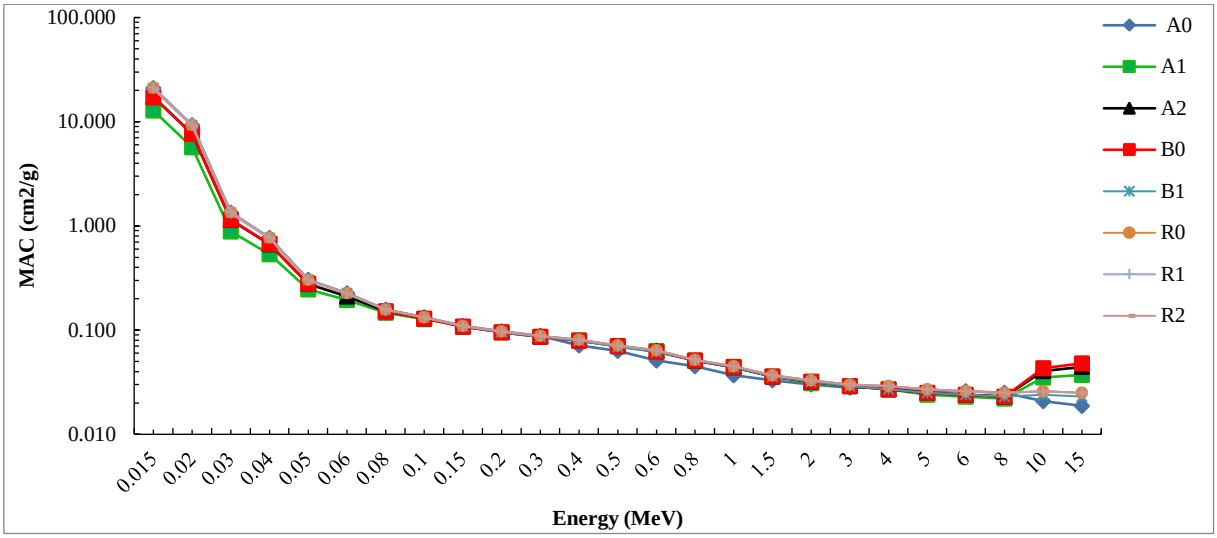

Fig. 1: Mass attenuation coefficient (MAC) for rocks samples

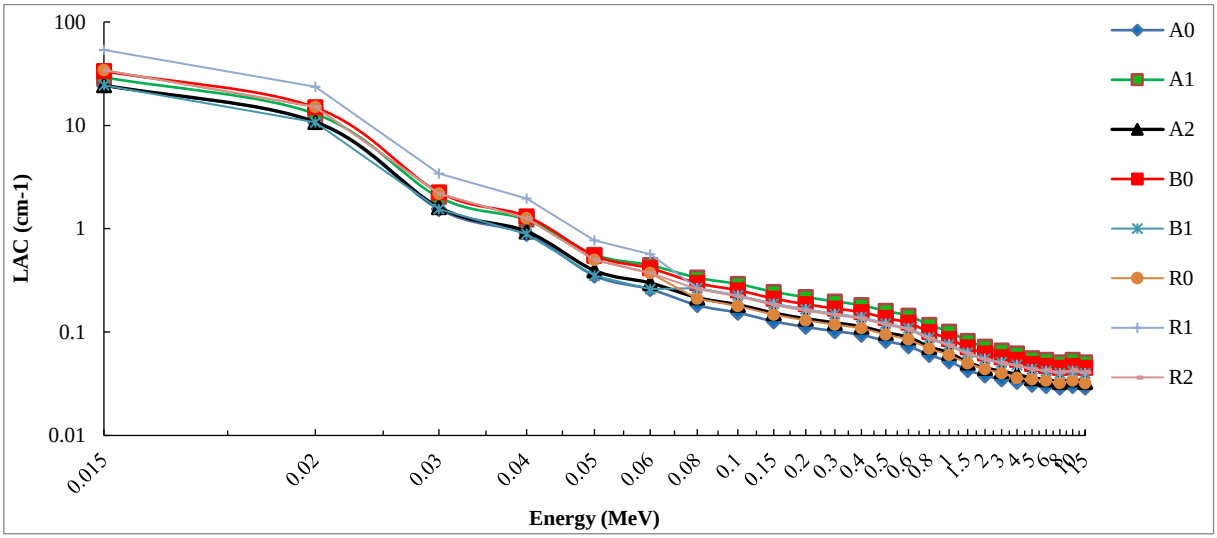

Fig. 2: Linear attenuation coefficient LAC For rocks samples.

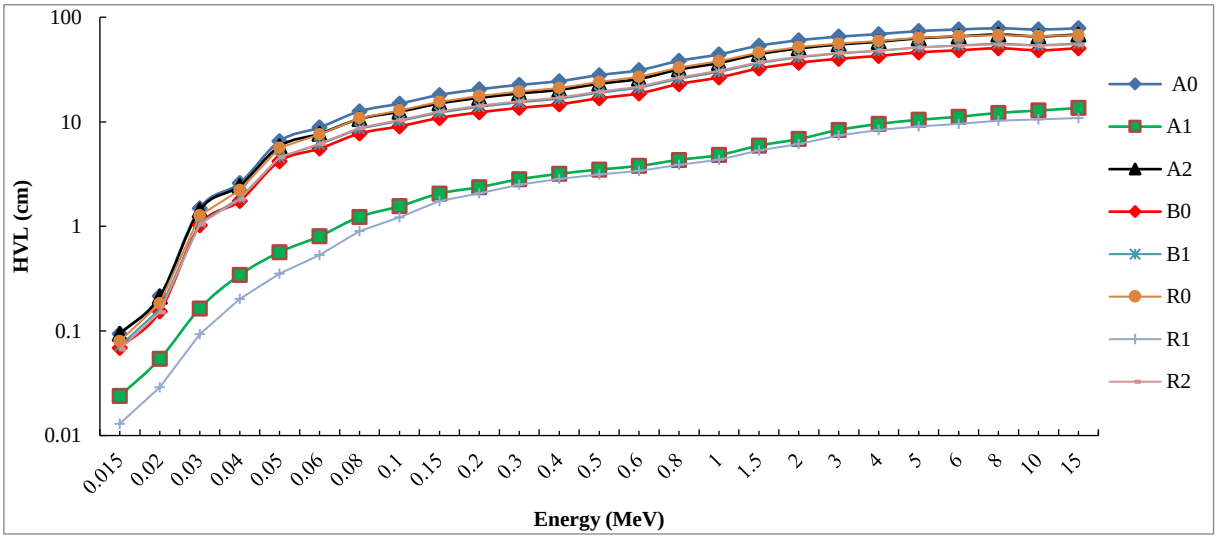

Fig. 3: Half value layer (HVL) for rocks samples

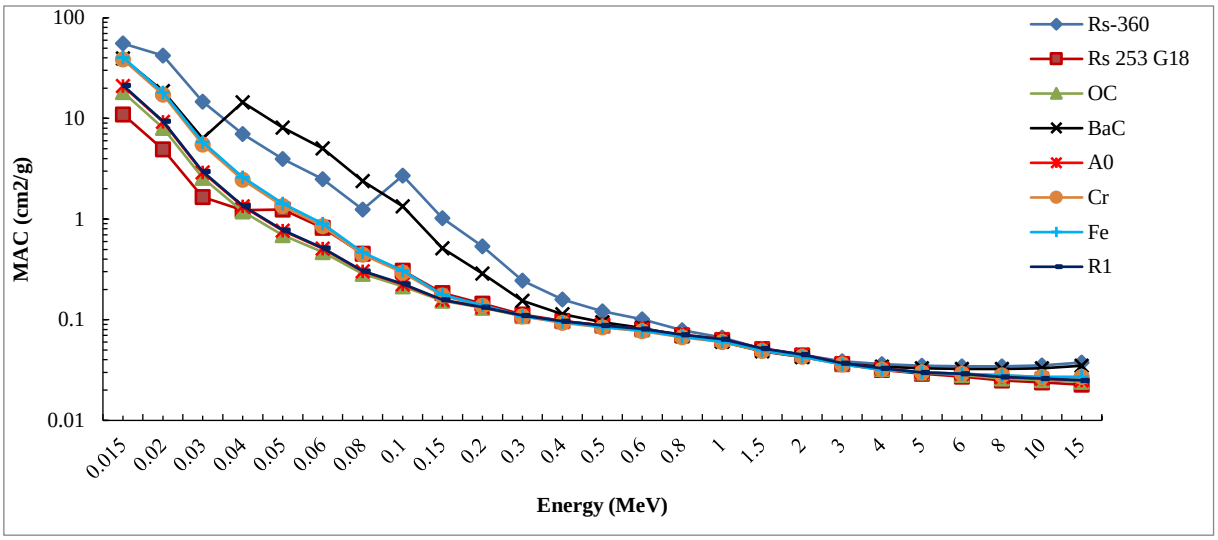

Fig. 4: Comparison of the MAC of A0 and R1 rocks with the other materials.

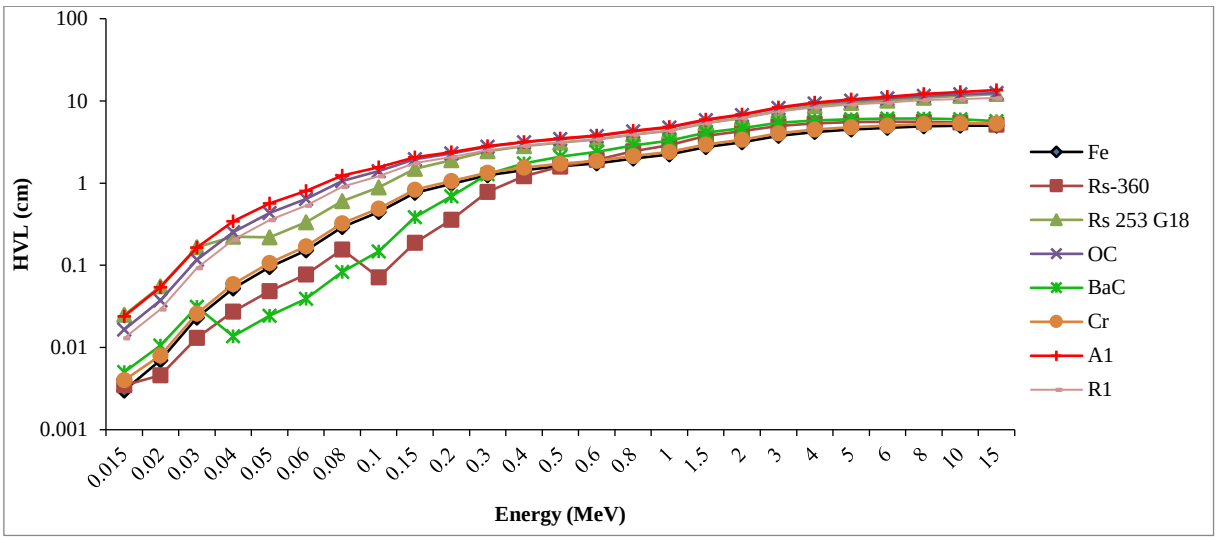

Fig. 5: Comparison of HVL for A1 and R1 samples with commercial materials.

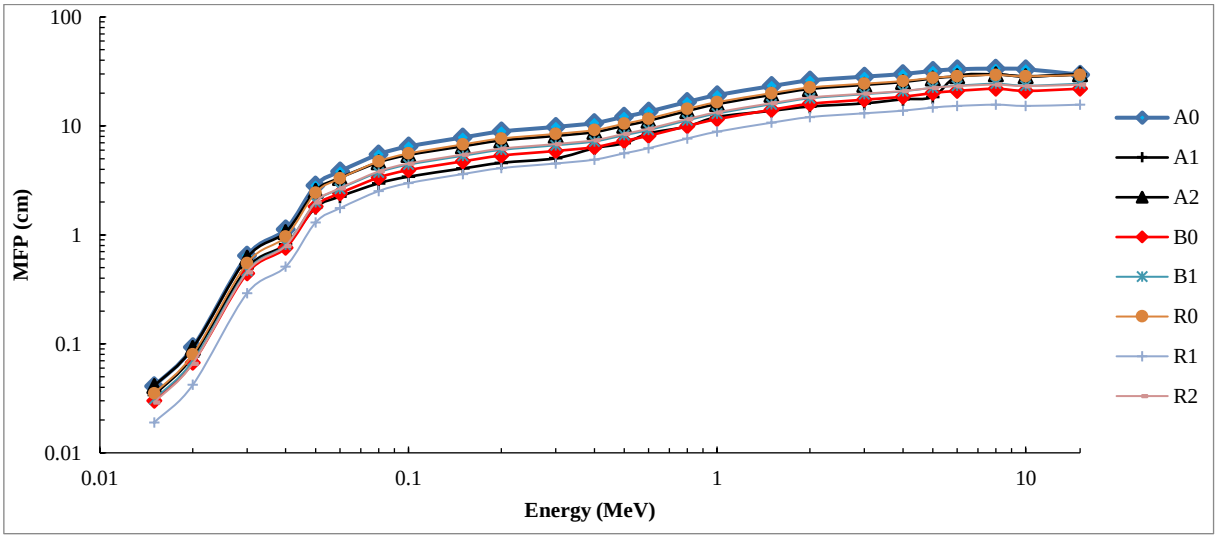

Fig. 6: Mean free path (MFP) for rocks samples.

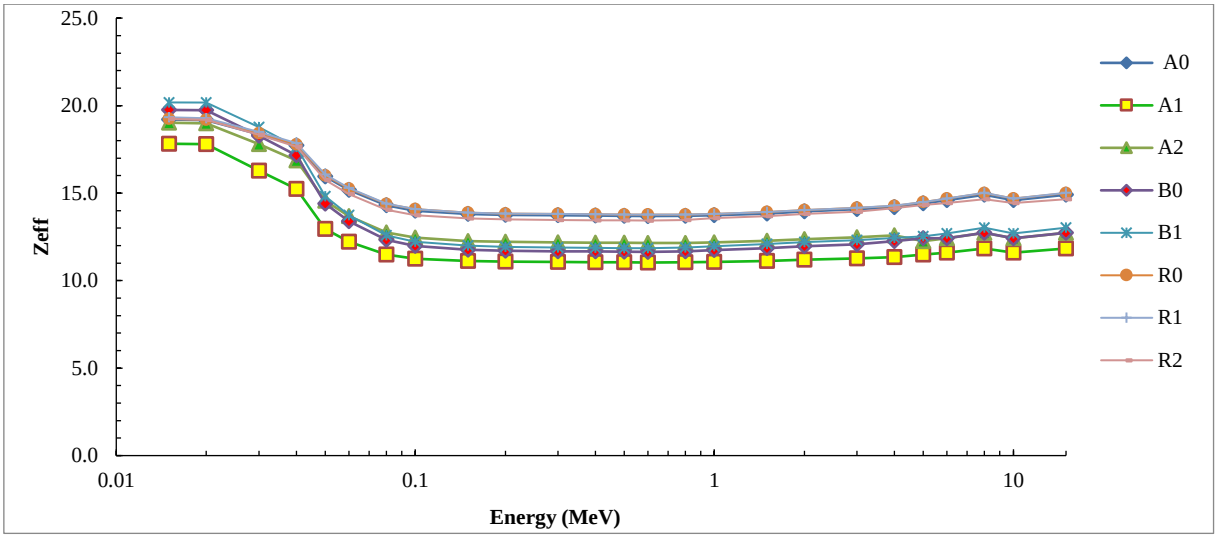

Fig. 7: The effective atomic number (Z_{eff}) calculated for rock samples.

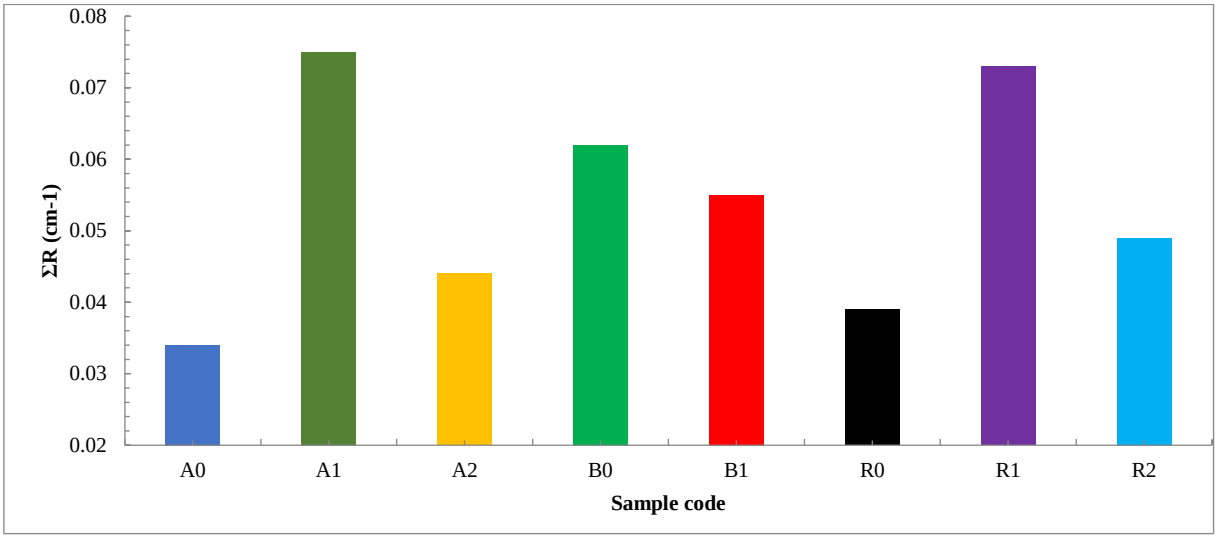

Fig. 8: Fast neutron removal cross section (FNRCS) for all samples.

مقالة بحثية

تقييم خصائص الحماية من إشعاع جاما والنيوترونات السريعة في مواد البناء اليمنية

سوسن عبدالله محمد[1]، ماهر طاهر حسين[2]، و عمران عيسى صالح[3،*]

[1] قسم الفيزياء، كلية التربية، جامعة ابين، اليمن
[2] قسم الفيزياء، كلية التربية، جامعة لحج، اليمن
[3] قسم الفيزياء، كلية العلوم، جامعة عدن، اليمن

* الباحث الممثّل: عمران عيسى صالح؛ البريد الالكتروني: eesas2009@yahoo.com

استلم في: 05 اكتوبر 2025 / قبل في: 01 ديسمبر 2025 / نشر في 31 ديسمبر 2025

المُلخّص

تم تقييم خصائص الحماية من إشعاع جاما لثمانية عينات من الصخور اليمنية (A0، A1، A2، B0، B1، R0، R1، وR2) عبر طيف طاقي للفوتونات يتراوح من 0.015 إلى 15 ميغا إلكترون فولت. تم حساب أهم معاملات الحماية النووية، ومنها معامل التوهين الكتلي (MAC)، وطبقة نصف السمك (HVL)، ومتوسط المسار الحر (MFP)، والعدد الذري الفعّال (Z_{eff}). أظهرت العينتان A0 وR1 أفضل أداء في الحماية؛ حيث بلغت قيم MAC لهما 21.0 و21.4 سم²/جرام عند طاقة 0.015 ميغا إلكترون فولت، متفوقةً على المواد التقليدية مثل الخرسانة العادية والزجاج التجاري Rs-360 وG18 Rs-253. كما كانت قيم HVL لهذه العينات منخفضة جداً، إذ بلغت 0.045 سم للعينة A0 و0.042 سم للعينة R1، مما يشير إلى قدرة عالية على التخفيف حتى بسمك قليل. وأكدت قيم MFP عند الطاقات المنخفضة الكفاءة العالية لتفاعل فوتونات جاما مع هذه العينات. أما العدد الذري الفعّال (Z_{eff}) فبلغ ذروته قرب 20 عند الطاقات المنخفضة، مما يعكس مساهمة فعالة للعناصر المكوّنة في امتصاص الفوتونات. مجتمعةً، تبيّن هذه النتائج أن عينتي A0 وR1 تمثلان مواد حماية فعالة جداً ضد إشعاع جاما، حيث تحتاجان إلى طبقات أرفع لتحقيق حماية مماثلة مقارنةً بالمواد التقليدية، مما يعزز إمكانيتهم كمادتي حماية طبيعية وذات تكلفة معقولة مناسبة للاستخدامات النووية والبنائية. من جهة اخرى تراوحت قيم المقطع العرضي للنيوترونات السريعة (ΣR) بين 0.034 و0.075 سم$^{-1}$، حيث أظهرت العينة A1 كفاءة فائقة في حجب النيوترونات السريعة. ومن المثير للاهتمام أن القيمة ΣR انخفضت مع زيادة كثافة العينة.

الكلمات المفتاحية: الحماية من إشعاع جاما؛ التوهين؛ العدد الذري؛ الصخور؛ طبقة نصف السمك (HVL).

How to cite this article:

S. A. Mohammed, M. T. Hausain, and E. E. Saleh, "EVALUATION OF GAMMA AND FAST NEUTRON SHIELDING PROPERTIES OF YEMENI BUILDING MATERIALS", *Electron. J. Univ. Aden Basic Appl. Sci.*, vol. 6, no. 4, pp. 225-234, Dec. 2025. DOI: https://doi.org/10.47372/ejua-ba.2025.4.474